New Behavioral-Level Simulation Technique for RF/Microwave Applications. Part I: Basic Concepts

S. L. Loyka[1,2], J. R. Mosig[3]

[1] LACIME-ETS, Ecole de Technologie Superieure, 1100, Notre-Dame St. West, Montreal (Quebec), H3C 1K3, Canada; e-mail: segey.loyka@ieee.org
[2] Belorussian State University of Informatics and Radioelectronics, P. Brovki St. 6, Minsk 220027, Belarus
[3] Swiss Federal Institute of Technology, LEMA-EPFL, Ecublens, CH-1015 Lausanne, Switzerland; e-mail: juan.mosig@epfl.ch

Received 16 November 1999; revised 3 April 2000

ABSTRACT: The quadrature modeling technique is nowadays widely used for the nonlinear simulation of RF/microwave communication circuits and systems at the behavioral (system) level. It allows one to simulate the circuit/system performance under real-world conditions and signals (using several thousand sample frequencies) and to predict such parameters as adjacent channel power ratio, spectral regrowth, and error vector magnitude in a computationally efficient way. But it is a narrowband technique and, consequently, cannot predict harmonics of the carrier frequency and even-order nonlinear products, to account for the circuit/system frequency response and the bias decoupling network effect. Here, we propose a new behavioral-level simulation technique (instantaneous quadrature technique) that overcomes these drawbacks, and demonstrate its validity through measurements and harmonic balance simulation. The transformation of envelope transfer characteristics into instantaneous ones is also discussed in detail. © 2000 John Wiley & Sons, Inc. Int J RF and Microwave CAE 10: 221–237, 2000.

Keywords: behavioral-level simulation; nonlinear modeling; quadrature technique

1. INTRODUCTION

Nowadays we observe an exponential increase in the number of RF and microwave communication systems and services. The complexity of communication circuits, systems, and signals has grown substantially during the past two decades, and this process is still going on. Due to limited spectrum and space available, new standards have been introduced in order to ensure an efficient spectrum utilization and the absence of inter- and intra-system interference and distortions. All these factors make the design process much more complex than, for example, two decades ago. Under these circumstances, computer-aided simulation is becoming a more and more important tool for the communication circuit/system design process (the historical perspective of this process can be observed using [1–6]). In general, we can classify modeling and simulation techniques into several groups:

1. Those based on fundamental physical laws (Maxwell's equations, etc.) [7–10].
2. Those based on circuit theory [11–18].
3. System-level methods (or "behavioral," or "black-box," or "input-output") [1–6, 18–22].
4. Multilevel (hybrid) methods that integrate various-level techniques [23–28].

Correspondence to: S. L. Loyka

First-group methods give the most detailed, complete, and accurate description of a circuit or system. But they are limited mainly due to limited computer resources: simulation time or the required computing power may be unreasonably large for a complex circuit, input signal, or electromagnetic environment ("You cannot solve Maxwell's equations for a CD player !"). Besides, the use of these methods requires very detailed characterization information that is not always available. In this case, second-group methods are needed. But they also work with some limitations due to the same reasons: one cannot simulate an entire mobile communication system or even a single-stage RF power amplifier with a digitally modulated input using a circuit-level method [harmonic balance (HB) technique or SPICE, for example] due to unpractically long simulation time and very high demand for computational power. In this case, third-group methods should be used. A combined use of all these methods can result in a very powerful multilevel analysis tool. Figure 1 shows an example of such a multilevel simulation method. The electromagnetic simulation and the circuit-level simulation are used in order to build behavioral models of the distributed part (an antenna, for example) and of the circuit (lumped-element) part of an entire system, correspondingly. The entire system is simulated at the behavioral level.

Nonlinear behavior of active stages (power or low-noise amplifiers, mixers, etc.) may severely degrade the overall communication system performance and, consequently, should be carefully analyzed in early phases of the design process. Behavioral-level simulation techniques are presently very popular for the nonlinear analysis of RF/microwave communication systems [1–6, 18, 19, 29–49]. They allow one to simulate the system behavior under a variety of real-world external conditions and system configurations in a computationally efficient way. Real-world digitally modulated signals are used for the simulation since single- or several-tone input signals do not characterize adequately the digital communication system behavior [18, 30–32]. Adjacent channel power ratio (ACPR), power spectrum regrowth (PSR), and error vector magnitude (EVM) are used for the assessment of nonlinear system performance since such parameters as intermodulation product (IMP) levels, intercept point, and spurious-free dynamic range (which are mainly used for analog systems) do not characterize adequately the digitally modulated system performance.

The quadrature modeling technique is the most popular tool for behavioral-level nonlinear modeling and simulation of active stages of RF/microwave circuits and systems [1, 18, 29–36]. This technique was introduced in the early 1970s for nonlinear modeling and simulation of traveling wave tube (TWT) amplifiers used in satellite communications [29]. It takes into account both amplitude-to-amplitude (AM–AM) and amplitude-to-phase (AM–PM) conversion (nonlinearity). At the present time, this technique is mainly used for the simulation of solid-state power amplifiers. This technique has many advantages: it allows one to simulate the power amplifier with a digitally modulated input signal using a PC in reasonable time and, consequently, to predict ACPR, PSR, and EVM. It can also predict IMPs and gain compression/expansion. The permissible number of input tones and the analysis dynamic range are quite large [18, 31, 32]. However, the main drawback of the quadrature modeling technique is that it is a narrowband one, so it cannot take into account frequency response, to predict harmonics of the carrier frequency and even-order nonlinear products, or to model the bias decoupling network

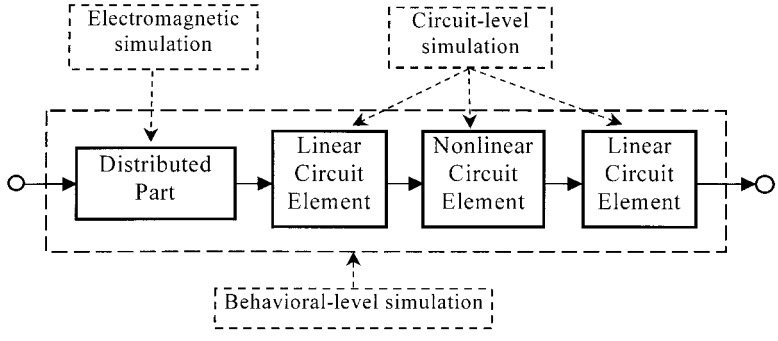

Figure 1. An example of multilevel simulation method.

effect [18, 32]. (Recently, some methods have been proposed to model the frequency response [33, 34, 36]; however, the nonlinear element is still modeled at the baseband level and, therefore, only the in-band frequency response can be modeled in this way.) The bias decoupling network effect limits the analysis accuracy even for narrowband signals and systems [32]. The quadrature modeling technique also uses an explicit representation of the modulated signal, so multiple-carrier signals cannot be simulated in a direct way.

The discrete technique was introduced in the 1980s for the nonlinear simulation of an RF/microwave receiving path taking into account nonlinear interference and distortions [37–42]. It also accounts for the spurious receiver channels (adjacent, image, local oscillator noise, etc.), IMPs and harmonics, gain compression/expansion, etc. The main application of this technique was to electromagnetic compatibility/ electromagnetic interference (EMC/EMI) analysis in a group of RF/microwave systems. An important advantage of the discrete technique is that instantaneous values of the signals are used during the analysis, not the complex envelope. Thus, the simulation is made over a wide frequency range. It allows one to predict harmonics and even-order nonlinear products, to take into account frequency response, and to analyze multicarrier systems. However, the discrete technique does not take into account AM–PM nonlinearity, which limits substantially the analysis accuracy. Both these techniques (the quadrature modeling technique and the discrete technique) are very computationally efficient as compared to circuit-level techniques (HB technique or SPICE), and still have a circuit-level accuracy in many cases.

In this paper, we consider these behavioral-level techniques in more detail, and propose a new one—an "instantaneous" quadrature technique—which uses advantages of both previous techniques. The practical requirement to a behavioral-level simulation technique used for RF/microwave applications is that it should provide narrowband as well as broadband analysis capabilities [to predict harmonics and to take into account input/output matching networks (filters)]; its analysis dynamic range should be in excess of 100 dB and frequency resolution should be better than 100 Hz [18]. We believe that the instantaneous quadrature technique can fulfill these requirements.

2. QUADRATURE MODELING TECHNIQUE

The main idea of the quadrature modeling technique is the use of a complex envelope instead of real narrowband signals [18, 29–32]. A real-life narrowband RF signal can be presented in the following form:

$$\begin{aligned} x(t) &= A(t)\cos(\omega_0 t + \varphi(t)) \\ &= \mathrm{Re}\{A(t)\cdot\exp[j\cdot(\omega_0 t + \varphi(t))]\}, \end{aligned} \quad (1)$$

where $A(t)$ and $\varphi(t)$ are amplitude and phase that vary slowly with respect to carrier (amplitude and phase modulation), and ω_0 is the carrier frequency. Its complex envelope is

$$\begin{aligned} \overline{A(t)} &= A(t)\cdot\exp[j\varphi(t)] \\ &= A(t)\cos\varphi(t) + jA(t)\sin\varphi(t). \end{aligned} \quad (2)$$

So, there is not any carrier information in the complex envelope, only modulation information (only the first harmonic zone is taken into account). It is very important from the viewpoint of computational efficiency, but it also limits the technique capabilities: only narrowband analysis is possible because the frequency response is assumed to be flat over the simulation bandwidth. Two terms on the right-hand side in (2) constitute in-phase and quadrature lowpass signals:

$$X_I(t) = A(t)\cos\varphi(t), \qquad X_Q(t) = A(t)\sin\varphi(t). \quad (3)$$

Figure 2 illustrates the complex envelope concept. The output signal of a bandpass nonlinear stage is

$$\begin{aligned} y(t) = K(A_{\mathrm{in}}(t))\cdot A_{\mathrm{in}}(t)\cdot\cos(\omega_0 t + \varphi_{\mathrm{in}}(t) \\ + \Phi(A_{\mathrm{in}}(t))), \end{aligned} \quad (4)$$

where A_{in} and φ_{in} are the input signal amplitude and phase. A nonlinear stage is characterized by its envelope amplitude and phase transfer factors:

$$K(A_{\mathrm{in}}) = \frac{A_{\mathrm{out}}}{A_{\mathrm{in}}}, \qquad \Phi(A_{\mathrm{in}}) = \varphi_{\mathrm{out}} - \varphi_{\mathrm{in}}. \quad (5)$$

$K(A_{\mathrm{in}})$ represents envelope AM–AM nonlinearity, and $\Phi(A_{\mathrm{in}})$ represents envelope AM–PM nonlinearity. Note that both factors depend on the input signal amplitude, not on the instantaneous value of the signal. This is due to the

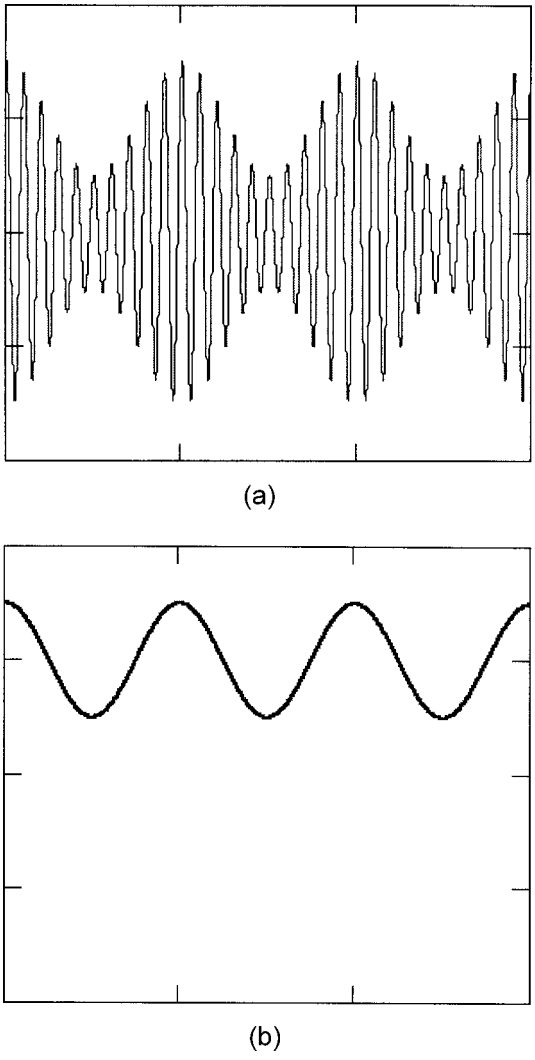

Figure 2. The complex envelope of an AM-modulated signal. (a) RF AM-modulated signal. (b) Its complex envelope [$\varphi(t) = 0$].

bandpass representation of signals and system stages (actually, lowpass equivalents of both are used). Thus, (5) constitutes the envelope nonlinearity. In the quadrature modeling technique, in-phase and quadrature envelope transfer factors are used:

$$K_I(A_{\text{in}}) = K(A_{\text{in}})\cos\Phi(A_{\text{in}}),$$
$$K_Q(A_{\text{in}}) = K(A_{\text{in}})\sin\Phi(A_{\text{in}}), \qquad (6)$$

and the output lowpass signal is expressed as

$$Y(t) = K_I(A_{\text{in}})X_I(t) - K_Q(A_{\text{in}})X_Q(t). \quad (7)$$

The modeling process can be illustrated by the block diagram shown in Figure 3. Note that two

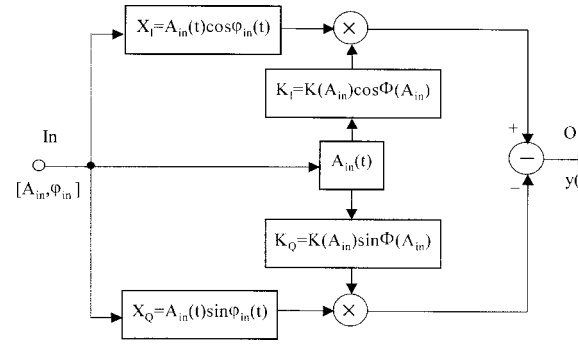

Figure 3. Modeling bandpass nonlinearity by the quadrature modeling technique.

independent channels (in-phase and quadrature) are used for the simulation. In this way, this technique takes into account both the AM–AM and the AM–PM nonlinearities. The nonlinear model of Figure 3 is sometimes called a memoryless nonlinearity [1]. Strictly speaking, this nonlinearity is not a memoryless one because there is a phase shift (AM–PM); thus, the output depends on the input at some past instants. (However, there is indeed no frequency dependence in this model.) The input of the quadrature nonlinearity is also shifted by $-\pi/2$ and this operation is not a memoryless one. (In fact, it is the Hilbert transform which is an integral transformation [1].) Consequently, this channel and the entire quadrature structure are not memoryless ones. However, we can still use the term "memoryless" in the sense that the transfer factors K_I and K_Q depend on the input signal amplitude A_{in} at the same instant only.

Unfortunately, the quadrature modeling technique is only valid for narrowband signals and systems (no harmonics or even-order nonlinearities). In its present form, it also cannot take into account frequency response (matching networks/filters) nor account for the bias decoupling network effect [32]. The modeling of multicarrier systems using this technique is possible (assuming a flat frequency response over the simulation bandwidth) [1], but it complicates the technique substantially and reduces its computational efficiency. Thus, some improvements are desirable. Such improvements will be discussed in Section 4.

3. DISCRETE TECHNIQUE

The basis of the discrete technique is a representation of the system block diagram as linear filters (matching networks) and memoryless nonlinear

elements (active elements) connected in series (or in parallel, or both) [37–49]. For example, Figure 4 shows a single-stage RF amplifier represented in this way (so-called "sandwiched" nonlinearity). Input and output filters can model input and output matching networks. This representation reflects characteristic peculiarities inherent to the construction of typical RF amplifying and converting stages. The utilization of the model with memoryless nonlinearity is not a significant limitation on the method. Nonzero memory effects can partially be factorized at the level of input or output filters; that is, this representation is equivalent with respect to the simulation of the "input-to-output" path.

Signal passage through a linear filter is simulated in the frequency domain using the complex transfer factor of the filter:

$$S_{\text{out}}(f_n) = S_{\text{in}}(f_n) \cdot K(f_n), \tag{8}$$

where $S_{\text{out}}(f_n)$ is the signal spectrum at the filter output, $S_{\text{in}}(f_n)$ is the signal spectrum at the filter input, $K(f_n)$ is the complex transfer factor of the filter, and f_n are sample frequencies. It is necessary to use an appropriate sampling technique in order to obtain a sampled spectrum [45, 66]. Signal passage through a nonlinear memoryless element is simulated in the time domain using the instantaneous transfer function of the element:

$$u_{\text{out}}(t_k) = F[u_{\text{in}}(t_k)], \tag{9}$$

where $u_{\text{out}}(t_k)$ is the instantaneous value of the output signal, $u_{\text{in}}(t_k)$ is the same for the input signal, t_k are sample points in time, and F is an instantaneous transfer function of the nonlinear element. This function can be calculated using the measured or circuit-level simulated AM–AM characteristic [29, 30, 48, 56–58] (see also Sec. 5). Some simple analytical or semi-empirical models of the transfer function can also be used, but the simulation accuracy is not very good in this case [44, 56, 59–61]. Note that the output of the nonlinear element depends on the input at the same instant. Thus, this nonlinearity is strictly memoryless.

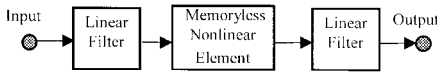

Figure 4. Single-stage RF amplifier in the discrete technique representation.

The transition from the time domain to the frequency domain and *vice versa* is made with the use of the direct and inverse fast Fourier transform (FFT) [50]:

$$S_n = \frac{1}{N}\sum_{k=0}^{N-1} u_k \cdot W^{nk}, \qquad u_k = \sum_{n=0}^{N-1} S_n \cdot W^{-nk}, \qquad W = e^{-j(2\pi/N)}, \tag{10}$$

where $S_n = S(f_n) = S(n\Delta f)$, $u_k = u(t_k) = u(k\Delta t)$; Δf is the frequency sample interval, Δt is the time sample interval, and N is the number of samples. It is worth mentioning that the normalization given in (10) must be used during the nonlinear analysis. The normalization of other types which is often used in the literature will produce incorrect results. The direct and inverse FFT vary only in the normalization and the exponent sign, which makes it possible to use the same algorithm to carry out the direct as well as the inverse FFT. It is necessary to make the corresponding data normalization and to arrange the data in the appropriate order before the FFT is carried out. Figure 5 illustrates broadband modeling of a typical RF active stage (power amplifier, for example) using the discrete technique.

Let us note a number of peculiarities connected with the use of the FFT for the nonlinear analysis.

1. The maximum frequency $F_{\max}$ in the signal spectrum, frequency sample interval Δf,

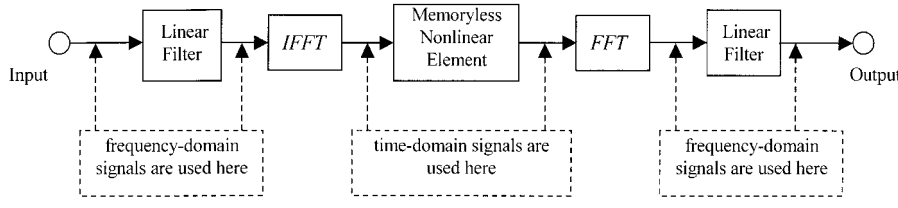

Figure 5. Modeling broadband nonlinearity by discrete technique. FET and IFFT are direct and inverse fast Fourier transforms.

time sample interval Δt, and the number of samples N (in time domain) are related by the following expressions (due to the Nyquist sampling theorem and FFT properties):

$$f_s = \frac{1}{\Delta t} = 2 \cdot F_{\max}, \quad N = \frac{T}{\Delta t} = \frac{f_s}{\Delta f}, \quad (11)$$

where $T = 1/\Delta f$ is the input signal period, and $f_s = 1/\Delta t$ is the sampling rate. The required number of samples in the frequency domain is actually equal to $N/2$, since samples with numbers arranged symmetrically with respect to $N/2$ are complex conjugate ones: $S_{N-n} = S_n^*$. In the time domain, all N samples are independent (but they are real numbers).

2. Nonlinear transformation of the input signal causes its spectrum to expand I times (I is the nonlinearity order). Therefore, taking into account the cyclic character of the FFT in the frequency domain [50], in order to avoid the spectrum aliasing distortion, the sampling rate must be at least [1]:

$$f_s = 2I \cdot F_{\max}. \quad (12)$$

However, from the practical viewpoint, this overestimates the sampling rate two ways. First, higher-order nonlinear components usually have smaller levels than do lower-order components and, consequently, will introduce relatively small aliasing distortion. Thus, one may use a lower sampling rate [than that given by (12)]. However, a particular choice of the sampling rate depends on a particular situation under consideration (on particular spectral components that must be taken into account, etc.). Second, we may be interested in calculating the output spectrum not up to $I \cdot F_{\max}$, but up to the same maximum frequency, $F_{\max}$, as at the input. In this case, (12) can be relaxed to

$$f_s = (I + 1) \cdot F_{\max}. \quad (13)$$

Strictly speaking, (12) and (13) are valid only for a polynomial (power series) transfer function of the nonlinear element. In this case, I is the polynomial order. However, we can also use a nonpolynomial representation of the nonlinear transfer function. (For example, a Bessel function expansion is a very effective tool for this purpose.) In this case, I is a safety factor. It should be determined in such a way that the spectrum aliasing effect does not disturb the required part of the output spectrum [1, 50, 62]. Practical values of I are about 5 to 50 depending on a specific scenario and a specific problem. When the inverse FFT is calculated at the nonlinear element output, the spectrum S_n has to be calculated only within the interval $[0, F_{\max}]$, which allows one to reduce the calculation time. The expressions (11)–(13) make it possible to determine the number of samples (and hence the amount of computer memory) which is required to analyze a system if the maximum frequency at the input, the frequency sample interval, and the order of nonlinearity (or the safety factor) are specified.

3. The dynamic range of amplitudes (the ratio of the maximum and minimum levels) in the signal spectrum is determined by errors in the signal amplitude quantization in the time domain, that is, by the accuracy of computer data presentation (for a typical floating-point number this value is about 280–300 dB). In order to achieve that high dynamic range, all the input signal spectral components must be rounded off to the sample frequencies (it is not a problem since a large number of sample frequencies can be used). Alternatively, some windows can be used when performing the FFT, but the dynamic range is limited in this case to 80–100 dB [63]. When simulating multistage systems, the quantization noise caused by the amplitude quantization is accumulated. This effect can be nullified by periodic "clearing" of the spectrum (that is, zeroing of the components whose level is lower than a certain threshold).
4. The utilization of nonuniformly spaced sample frequencies [51–53] makes it possible to reduce the number of samples, or to reduce the frequency sample interval, or to increase the order of simulated nonlinearity. However, it will slightly increase the simulation time.

Further improvement in the computational efficiency of the simulation can be achieved by means of a two-stage simulation scheme [41]. At the first stage, the simulation correct to the carrier frequencies (low frequency resolution) is carried out. All interference signals revealed at the first stage

are sequentially analyzed at high frequency resolution (correct to the modulating spectra) and with transformation to low frequencies (the sampling frequency is substantially reduced in this way).

It should be emphasized that the instantaneous values of signals are used in the discrete technique. Thus, it allows one to carry out simulation over a wide frequency range (for instance, to predict harmonics of the fundamental frequency and even-order nonlinear products). Frequency response can also be taken into account in this way. Unfortunately, the discrete technique also has drawbacks: it cannot take into account the AM–PM nonlinearity. Thus, some combination of the discrete and quadrature modeling techniques is desirable.

4. INSTANTANEOUS QUADRATURE TECHNIQUE

The main idea of the combined technique—the "instantaneous" quadrature technique—is to use advantages of both techniques and to build a hybrid technique [48, 49]. In order to model signals and systems over a wide frequency range, the instantaneous values of the signals must be used, not the complex envelope. In order to model the AM–PM conversion, the quadrature modeling structure should be used for the nonlinear element modeling. Thus, the modeling process consists of the following items:

1. Linear filters are modeled in the frequency domain (the same as for the discrete technique).
2. Nonlinear elements are modeled in the time domain using the quadrature structure, but the instantaneous signal values are used, not the complex envelope.
3. The transform from the frequency (time) domain to the time (frequency) domain is made by IFFT (FFT) (very computationally efficient).
4. The Hilbert transform [1, 64] is used to calculate in-phase and quadrature components:

$$x_Q(t) = \hat{x}(t) = \int_{-\infty}^{\infty} \frac{x(\tau)}{t-\tau}\, d\tau,$$
$$x_I(t) = x(t), \qquad (14)$$

where $x_I(t)$ and $x_Q(t)$ are instantaneous in-phase and quadrature components of the signal, and $\hat{x}(t)$ is the Hilbert-conjugate signal of $x(t)$. In fact, we use the Hilbert transform in the frequency domain to calculate the quadrature components because it does not require numerical integration and, thus, is much more computationally efficient:

$$x_Q(t) = \mathrm{IFFT}(-j \cdot S(\omega)) \quad \text{for } \omega \geq 0,$$
$$S(\omega) = \mathrm{FFT}(x(t)), \qquad (15)$$

where $S(\omega)$ is the signal's spectrum. The signal itself is the in-phase component, and the Hilberts-conjugate signal is the quadrature component.

Figure 6 gives an illustration of the nonlinear element modeling (S_{in} and S_{out} are input and output spectra, k_I and k_Q are the instantaneous in-phase and quadrature transfer factors; see Sec. 5 for more detail). It should be noted that the transfer function of the quadrature channel is not a usual transfer function in a conventional sense: it depends not only on the input of the quadrature nonlinearity (x_Q) but also on the input of the entire structure (x_{in}) i.e., on the input of the in-phase nonlinearity (x_I). Consequently, we cannot use the usual methods of the transformation of the envelope transfer function into the instantaneous one [29, 57] (see also Sec. 5). At the same time, the transfer function of the in-phase channel is a usual transfer function and those methods can be applied in this case.

An illustration of the modeling process is shown in Figure 7. We use the term "quasi-memoryless nonlinearity" in the sense that the instantaneous transfer factors depend on the instantaneous input signal level at the same instant. In general, this nonlinearity is not a memoryless one due to the Hilbert transform used in the quadra-

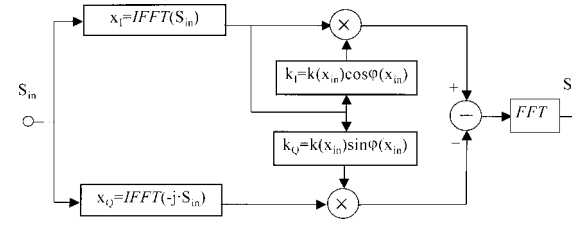

Figure 6. Modeling broadband nonlinear element by the "instantaneous" quadrature technique. S_{in} and S_{out} are the input and output spectra.

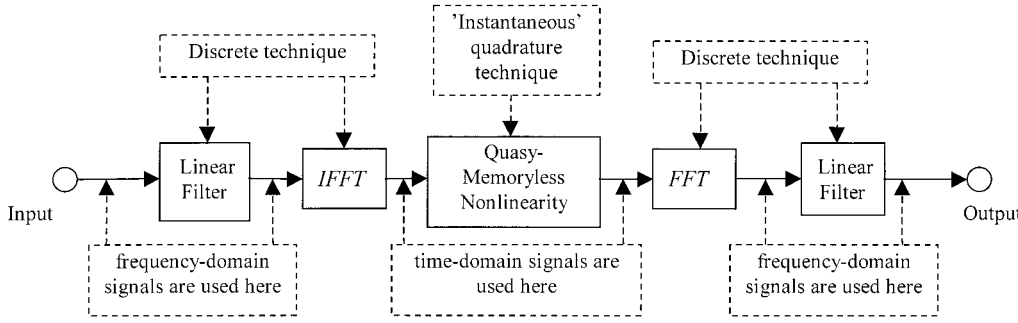

Figure 7. Simulating a single-stage radio amplifier by the instantaneous quadrature technique.

ture channel [see (14)]. Thus, the output of this channel depends on the input not only at the same instant, but also at all other instants in the past as well as in the future (corresponds to the integration over infinite time interval). However, for a narrowband RF signal, the output depends effectively only on the input at the same instant and at some nearby instants [65]; thus, the memory is really very small (however, not zero due to the AM–PM conversion). The nonlinearity is completely memoryless when there is no AM–PM conversion at all and the quadrature channel can be omitted.

It is not so easy to factorize the measured frequency response into the input and output filters' responses. The simplest way to solve this problem is to consider them to be equal (we used this approach in our simulation examples given in Sec. 6). However, the accuracy of this method is not very good in many instances (especially for the even-order nonlinearities). An alternative way is to simulate these responses at the circuit level, or to use some theoretical considerations for the factorization of the entire frequency response.

It should be emphasized that the instantaneous transfer factors $k_I(x_{\text{in}})$ and $k_Q(x_{\text{in}})$ are used for the simulation, not the envelope ones. The calculation of these factors will be considered in the next section.

5. INSTANTANEOUS TRANSFER CHARACTERISTICS

In this section, we consider how to determine the instantaneous transfer factors (k_I and k_Q) using the envelope transfer factors (K_I and K_Q) which can be measured or simulated by a circuit-level simulator (SPICE or HB-technique simulator, for example).

First of all, it should be noted that the instantaneous transfer factors consist of even and odd parts:

$$k_I(x_{\text{in}}) = k_{I,\text{even}}(x_{\text{in}}) + k_{I,\text{odd}}(x_{\text{in}}),$$
$$k_Q(x_{\text{in}}) = k_{Q,\text{even}}(x_{\text{in}}) + k_{Q,\text{odd}}(x_{\text{in}}). \quad (16)$$

In a narrowband analysis, the odd parts are usually omitted and only the even parts are considered. (We recall that the odd part of the transfer factor corresponds to the even part of the transfer function and *vice versa* for the even part; the transfer function is the transfer factor multiplied by the input signal.) However, we consider here a broadband analysis technique; thus, the odd parts must be taken into account (in order to predict even-order nonlinear products). Besides, the odd parts of the transfer factors can give a substantial contribution to odd-order nonlinear products due to the bias decoupling network effect [32].

Second, we should note that the same mathematical formulation cannot be used for the calculation of the in-phase and quadrature instantaneous transfer factors (using, for example, methods given in [57] or [29])—one needs two different formulations. Some mathematical techniques have been proposed in the past for transferring the envelope transfer function into the instantaneous one [29, 57]. However, these techniques are valid for the in-phase functions only and are quite complicated from a computational viewpoint.

Below, we discuss a general transformation method which is valid for the in-phase as well as quadrature factors and for both the even and odd parts, and how to apply the powerful method of moments approach for the calculation of the instantaneous transfer factors. In Section 5.1, we consider the determination of the even parts first,

omitting the subscript "even" for simplicity. After this, in Section 5.2, we shall consider the determination of the odd parts in a similar way.

5.1. Even Part of the Instantaneous Transfer Factors

Using the instantaneous quadrature modeling structure (see Fig. 6), we can present the output signal in the following form:

$$x_{\text{out}}(t) = x_{\text{in}}(t)k(x_{\text{in}})\cos(\varphi(x_{\text{in}})) - \hat{x}_{\text{in}}(t)k(x_{\text{in}})\sin(\varphi(x_{\text{in}})). \quad (17)$$

For a single-tone input,

$$x_{\text{in}}(t) = A_{\text{in}}\cos(\omega \cdot t), \quad (18)$$

(we assume $\varphi_{\text{in}} = 0$ without loss of generality), one obtains

$$x_Q(t) = \hat{x}_{\text{in}}(t) = A_{\text{in}}\sin(\omega \cdot t). \quad (19)$$

Let us consider the first harmonic zone component at the output:

$$x_{\text{out},1}(t) = A_{\text{out}}\cos(\omega \cdot t + \Phi). \quad (20)$$

Using this component, we can determine only the even part of the transfer factors in the following way. Employing the Fourier transform, we obtain the following expressions for the first-zone output amplitude and phase:

$$A_{\text{out}} = \sqrt{a_1^2 + b_1^2}, \qquad \Phi = \tan^{-1}\left(\frac{b_1}{a_1}\right), \quad (21)$$

where

$$a_1 = \frac{2}{T}\int_{-T/2}^{T/2} x_{\text{out}}(t)\cos(\omega \cdot t)\,dt,$$

$$b_1 = \frac{2}{T}\int_{-T/2}^{T/2} x_{\text{out}}(t)\sin(\omega \cdot t)\,dt, \quad (22)$$

and $T = 1/\omega$. After some mathematical development, we arrive at the following expressions:

$$\frac{4}{\pi}\int_0^{\pi/2} k_I(A_{\text{in}}\cos(x))\cos^2(x)\,dx = K_I(A_{\text{in}}), \quad (23a)$$

$$\frac{4}{\pi}\int_0^{\pi/2} k_Q(A_{\text{in}}\cos(x))\sin^2(x)\,dx = K_Q(A_{\text{in}}), \quad (23b)$$

where K_I and K_Q are given by (6). Note that (23a) and (23b) are not the same. Thus, one cannot use the same method of transferring $K \to k$ for the in-phase and quadrature factors (as was proposed in [29]).

We can determine $K_I(A_{\text{in}})$ and $K_Q(A_{\text{in}})$ from measurements or circuit-level simulation (AM–AM and AM–PM). Thus, (23) is in fact a system of two integral equations: we must find $k_I(x_{\text{in}})$ and $k_Q(x_{\text{in}})$ for given $K_I(A_{\text{in}})$ and $K_Q(A_{\text{in}})$. We can solve this system of integral equations purely numerically using the method of moments [7]. However, if we use a large number of sample points (and we have to do so in order to obtain a satisfactory accuracy—we consider this issue in more detail in the second part of this paper), the computational resources required and the computational time can be too large. Thus, we propose to use the following semi-analytical method. First, we transform (23) to the following form:

$$\frac{4}{\pi}\int_0^1 k_I(A_{\text{in}}t)\frac{t^2}{\sqrt{1-t^2}}\,dx = K_I(A_{\text{in}}),$$

$$\frac{4}{\pi}\int_0^1 k_Q(A_{\text{in}}t)\sqrt{1-t^2}\,dx = K_Q(A_{\text{in}}). \quad (24)$$

Then, using the traditional method of moments approach [7], we discretize (24) (piecewise constant basis functions and the point matching technique are used) and transform it to the two systems of linear equations:

$$\sum_{i=1}^{j} k_{I,i}A_{ij} = K_{I,j}, \qquad \sum_{i=1}^{j} k_{Q,i}B_{ij} = K_{Q,j},$$

$$j = \overline{1,N}, \quad (25)$$

where

$$k_{I,i} = k_I(A_{\text{in}} t_i), \qquad k_{Q,i} = k_Q(A_{\text{in}} t_i),$$
$$t_i = \frac{i - 1/2}{N}, \qquad i = \overline{1, N}, \tag{26}$$

$$K_{I,j} = K_I(A_{\text{in},j}), \qquad K_{Q,j} = K_Q(A_{\text{in},j}),$$
$$A_{\text{in},j} = A_{\text{in,max}} \frac{j}{N}, \tag{27}$$
$$j = \overline{1, N}, \qquad A_{\text{in}} \in [0, A_{\text{in,max}}],$$

$$A_{ij} = \frac{2}{\pi}(a_{ij} - a_{i-1,j} + b_{i-1,j} - b_{ij}),$$
$$a_{ij} = \sin^{-1}\left(\frac{i}{j}\right),$$
$$B_{ij} = \frac{2}{\pi}(a_{ij} - a_{i-1,j} + b_{ij} - b_{i-1,j}),$$
$$b_{ij} = \frac{i}{j}\sqrt{1 - \left(\frac{i}{j}\right)^2}$$
$$i \le j, \qquad i, j = \overline{1, N}, \tag{28}$$

and $A_{\text{in,max}}$ is the maximum amplitude of the input signal ($K_I(A_{\text{in}})$ and $K_Q(A_{\text{in}})$ are defined in the range $A_{\text{in}} \in [0, A_{\text{in,max}}]$), and N is the number of sample points used for the discretization of (24). Further, we observe that matrixes A_{ij} and B_{ij} are upper triangular ones. Consequently, (25) can be solved analytically in a recurrent form:

$$k_{I,1} = K_{I,1}, \qquad k_{Q,1} = K_{Q,1},$$
$$k_{I,j} = \frac{K_{I,j} - \sum_{i=1}^{j-1} k_{I,i} A_{ij}}{A_{jj}},$$
$$k_{Q,j} = \frac{K_{Q,j} - \sum_{i=1}^{j-1} k_{Q,i} B_{ij}}{B_{jj}},$$
$$j = \overline{2, N}. \tag{29}$$

Thus, we do not need to invert numerically the matrixes A_{ij} and B_{ij} that make this method much more computationally efficient than the traditional approach. Despite their rather complicated form, (25)–(29) can be easily and efficiently evaluated using a computer. In order to get a satisfactory accuracy, we have to use a large number of sample points: practically, N is 100 to 1000 depending on specific AM–AM and AM–PM data.

AM–AM and AM–PM characteristics which we need to calculate $k_I(x_{\text{in}})$ and $k_Q(x_{\text{in}})$ can be measured or simulated using a circuit-level simulator in a standard way. We should note, however, that the accuracy of AM–AM and AM–PM measurement or simulation is of primary importance: since we deal with a nonlinear problem, even small inaccuracies in AM–AM and/or AM–PM can result in a large inaccuracy in the final simulation results (IMP or harmonic levels, for example). Thus, special attention must be paid to this issue (we consider this in more detail in the second part of this paper).

We should also note that there are also two quasi-analytical methods to calculate the instantaneous transfer factors using (1) the Bessel function expansion, and (2) the polynomial expansion of the envelope transfer characteristics.

In the first method [29], we define in-phase and quadrature envelope transfer characteristics for a single-tone input [see (18)] in the following way:

$$A_{\text{out},I}(A_{\text{in}}) = A_{\text{out}} \cos(\Phi),$$
$$A_{\text{out},Q}(A_{\text{in}}) = A_{\text{out}} \sin(\Phi). \tag{30}$$

Further, we expand $A_{\text{out},I}$ and $A_{\text{out},Q}$ in a Bessel function series:

$$A_{\text{out},I}(A_{\text{in}}) = \sum_{n=\text{odd}} a_{I,n} J_1(n\xi A_{\text{in}}),$$
$$A_{\text{out},Q}(A_{\text{in}}) = \sum_{n=\text{odd}} a_{Q,n} J_1(n\xi A_{\text{in}}), \tag{31}$$

where J_1 is the first-order Bessel function of the first kind, and

$$\xi = \frac{\pi}{2A_{\text{in,max}}}. \tag{32}$$

The least-squares curve-fitting method together with the singular value decomposition technique (SVD) should be used for such an expansion [50] because Bessel functions are not orthogonal. Then the instantaneous transfer factors can be expressed as [it can be verified using (23)]:

$$k_I(x_{\text{in}}) = \sum_{n=\text{odd}} \frac{n\xi}{2} a_{I,n} \frac{\sin(n\xi x_{\text{in}})}{n\xi x_{\text{in}}},$$
$$k_Q(x_{\text{in}}) = \sum_{n=\text{odd}} \frac{n\xi}{2} a_{Q,n} \cos(n\xi x_{\text{in}}), \tag{33}$$

where n is an odd integer.

The second method [56] allows one to calculate only the in-phase instantaneous transfer factor (however, the odd part of the transfer factor can also be calculated by this method). In this method, we expand $A_{\text{out},I}$ in a power series (the least-squares curve-fitting method and the SVD technique should also be used) assuming that $A_{\text{out},I}(-A_{\text{in}}) = -A_{\text{out},I}(A_{\text{in}})$ (since we consider the even part of the transfer factor):

$$A_{\text{out},I}(A_{\text{in}}) = \sum_{n=\text{odd}} a_n A_{\text{in}}^n. \tag{34}$$

Further, the in-phase instantaneous transfer factor can be expressed as:

$$k_I(x_{\text{in}}) = \sum_{n=\text{odd}} a_n \frac{2^{n-1}}{C_n^{(n-1)/2}} x_{\text{in}}^{n-1}, \tag{35}$$

where C_n^m are the binomial expansion coefficients.

5.2. Odd Part of the Instantaneous Transfer Factors

Odd parts of the instantaneous transfer factors can be determined in a similar way, using the second-order envelope characteristics (second harmonic zone AM–AM and AM–PM functions or second-order IMP at the output for the two-tone input). In this paper, we use the second harmonic zone (second-order) AM–AM and AM–PM (we also omit the subscript "odd" for simplicity). In this case, (23) takes the form:

$$\begin{aligned}
&\frac{4}{\pi}\int_0^{\pi/2} k_I(A_{\text{in}}\cos(x))\cos(x)\cos(2x)\,dx \\
&\qquad = K_{I,2}(A_{\text{in}}), \\
&\frac{4}{\pi}\int_0^{\pi/2} k_Q(A_{\text{in}}\cos(x))\sin(x)\sin(2x)\,dx \\
&\qquad = K_{Q,2}(A_{\text{in}}),
\end{aligned} \tag{36}$$

where $K_{I,2}(A_{\text{in}})$ and $K_{Q,2}(A_{\text{in}})$ are the second-order envelope transfer factors,

$$\begin{aligned}
K_{I,2}(A_{\text{in}}) &= \frac{A_{\text{out},2}}{A_{\text{in}}}\cos(\Phi_2(A_{\text{in}})), \\
K_{Q,2}(A_{\text{in}}) &= \frac{A_{\text{out},2}}{A_{\text{in}}}\sin(\Phi_2(A_{\text{in}})),
\end{aligned} \tag{37}$$

and $A_{\text{out},2}$ and Φ_2 are the second-order AM–AM and AM–PM. We can also solve the integral equations (36) using the traditional method of moments approach. But, as practical experience shows, it requires even more sample points than for the even parts. Thus, we use the semi-analytical approach proposed in Section 5.1. First, we transform (36) to the form:

$$\begin{aligned}
&\frac{4}{\pi}\int_0^1 k_I(A_{\text{in}}t)\frac{t(2t^2-1)}{\sqrt{1-t^2}}\,dx = K_{I,2}(A_{\text{in}}), \\
&\frac{8}{\pi}\int_0^1 k_Q(A_{\text{in}}t)t\sqrt{1-t^2}\,dx = K_{Q,2}(A_{\text{in}}).
\end{aligned} \tag{38}$$

Then we discretize these integral equations and obtain two systems of linear equations:

$$\begin{aligned}
&\sum_{i=1}^{j} k_{I,i}A_{ij} = K_{I,2,j}, \qquad \sum_{i=1}^{j} k_{Q,i}B_{ij} = K_{Q,2,j}, \\
&\qquad j = \overline{1,N},
\end{aligned} \tag{39}$$

where $k_{I,i}(x_{\text{in}})$ and $k_{Q,i}(x_{\text{in}})$ are determined by (26), $K_{I,2,i}(A_{\text{in}})$ and $K_{Q,2,i}(A_{\text{in}})$ are determined by (27) (K_I and K_Q are substituted by $K_{I,2}$ and $K_{Q,2}$, correspondingly), and

$$\begin{aligned}
A_{ij} &= \frac{8}{3\pi}(b_{i-1,j}\cdot a_{i-1,j} - b_{ij}\cdot a_{ij}), \\
a_{ij} &= \frac{1}{2} + \left(\frac{i}{j}\right)^2, \\
B_{ij} &= \frac{8}{3\pi}\left(b_{i-1,j}^3 - b_{i,j}^3\right), \qquad b_{ij} = \sqrt{1-\left(\frac{i}{j}\right)^2}, \\
&\qquad i \le j, \qquad i,j = \overline{1,N}.
\end{aligned} \tag{40}$$

Further, (39) is solved analytically in a recurrent form given by (29).

We can also use the quasi-analytical method [56] to calculate the odd part of the in-phase instantaneous transfer factor. To do so, we define the second-order in-phase envelope transfer characteristic as:

$$A_{\text{out},2,I}(A_{\text{in}}) = A_{\text{out},2}\cos(\Phi_2(A_{\text{in}})). \tag{41}$$

Then, we expand $A_{\text{out},2,I}$ in a power series assuming that $A_{\text{out},2,I}(-A_{\text{in}}) = A_{\text{out},2,I}(A_{\text{in}})$ (since

we are looking for the odd part of the transfer factor):

$$A_{\text{out},2,I}(A_{\text{in}}) = \sum_{n=\text{even}>0} a_n A_{\text{in}}^n, \qquad (42)$$

where n is an even integer. Further, the in-phase instantaneous transfer factor can be expressed as:

$$k_I(x_{\text{in}}) = \sum_{n=\text{even}>0} a_n \frac{2^{n-1}}{C_n^{n/2-1}} x_{\text{in}}^{n-1}. \qquad (43)$$

In order to determine the odd part of the instantaneous transfer factors by these methods, we need to know the second-order envelope transfer characteristics, $A_{\text{out},2}(A_{\text{in}})$ and $\Phi_2(A_{\text{in}})$. One can simulate these characteristics using a circuit-level simulator (for example, SPICE or HB-based simulator) in a simple way. But the measurement of these characteristics is not so simple. First of all, we can measure the envelope transfer characteristic ($A_{\text{out},2}(A_{\text{in}})$) using a conventional measurement setup comprised of a signal generator and a spectrum analyzer, but we can not measure the phase characteristic ($\Phi_2(A_{\text{in}})$) in this way. For this purpose, one can use an approach similar to one proposed in [54]. In this approach, we use two independent paths —a primary path including first variable attenuator, device under test (DUT), second variable attenuator, and variable phase shifter, and a reference path including a reference second harmonic (H_2) generator (see Fig. 8). The input signal at the H_2 generator is kept constant during measurements. Thus, at its output we have the second harmonic of a constant level and phase (which is used as a reference). The level of the DUT input signal is changed using the first variable attenuator. The second variable attenuator and phase shifter are used to minimize the spectral level of H_2 at the spectrum analyzer input. In this way, we can measure the second order transfer characteristics ($A_{\text{out},2}(A_{\text{in}})$ and $\Phi_2(A_{\text{in}})$) as functions of the signal level at the DUT input.

As for the case of first-order AM–AM and AM–PM, special care must be paid to the accuracy of $A_{\text{out},2}(A_{\text{in}})$ and $\Phi_2(A_{\text{in}})$ measurement or simulation due to the nonlinear character of the problem.

6. VALIDATION OF THE INSTANTANEOUS QUADRATURE TECHNIQUE

In order to validate the technique proposed, extensive circuit-level simulations and measurements have been made. Below, we give some simulation examples for microwave amplifiers. Figures 9 and 10 show gain (AM–AM) and output signal relative phase (AM–PM) versus input signal level for a single-stage transistor microwave amplifier, which were simulated by the harmonic balance technique (HP Advanced Design System was used [55]). Note that envelope and instantaneous characteristics differ (it is especially obvious for the AM–PM characteristics). Further, we shall consider HB simulation results as a reference because its accuracy is in general better (since it is a circuit-level simulation; we should note, however, that it also has a lot of limitation, especially for nonlinear problems). The instantaneous characteristics were calculated using (29). Figure 11 shows fundamental tone and IMP levels at the amplifier output (two-tone input signal was used), which were simulated by the instantaneous quadrature technique (see Figures 6 and 7) and by the HB technique [55]. Agreement between HB simulation and the technique proposed is very good except for fifth- and higher-order IMPs in the small-signal area (< -10 dBm), which

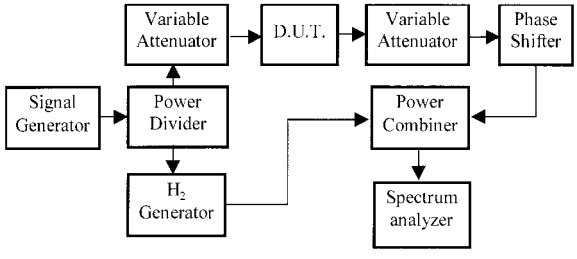

Figure 8. Block diagram for the measurement of second-order AM–AM and AM–PM.

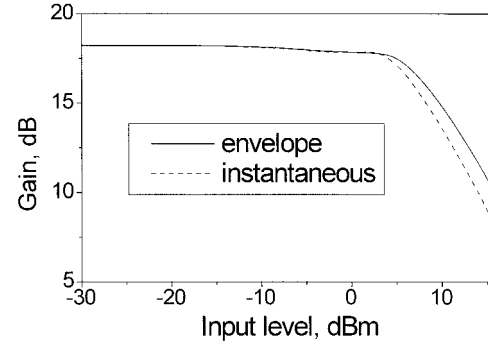

Figure 9. Envelope and instantaneous gains versus input level.

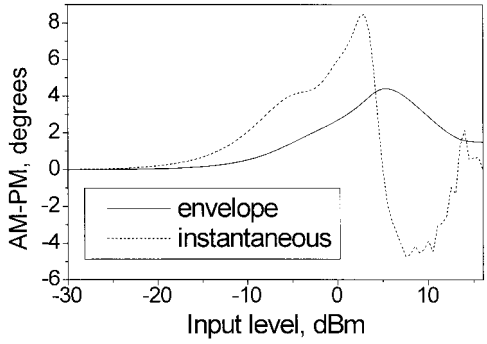

Figure 10. Envelope and instantaneous AM–PM characteristics versus input level.

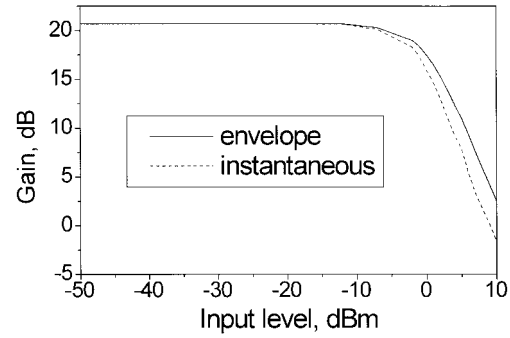

Figure 12. Envelope (solid line) and instantaneous (dotted line) gains versus input level.

requires further investigation. Note that the correct prediction of the fundamental component also proves that the transformation method of the envelope transfer function into instantaneous ones is correct.

We should point out that the dynamic range of the simulation is very high (from −150 dBm up to 20 dBm, i.e., 170 dB). The instantaneous quadrature technique is also very computationally efficient: simulation time for this technique is only a few minutes; for the HB technique it is more than 5 hours. This difference becomes even larger for a larger number of input tones (for, say, 1000 input tones the HB simulation would last for an unreasonably long time; the simulation time of the instantaneous quadrature technique does not roughly depend on the number of input tones).

Figure 12 shows the gain of a microwave monolithic integrated circuit (MMIC) amplifier versus input signal level (AM–AM). The envelope gain was measured and the instantaneous gain was calculated using (29). AM–PM characteristic was not taken into account due to its small values. Figure 13 shows fundamental tone and harmonics at the amplifier output, which were measured and simulated by the instantaneous quadrature technique. This figure illustrates the capability of this technique to perform simulation over a wide frequency range (to predict harmonics) and over a wide dynamic range at the same time. Figure 14 illustrates a desensitization in the amplifier (this phenomenon may be important for the EMC/EMI analysis of a communication system). There is a two-tone input (one tone is a required signal of a fixed amplitude, and the other is an interfering signal of varying amplitude) and the figure shows the required and interfering signals at the output versus the interfering signal amplitude at the input. The technique proposed predicts the amplifier performance quite well even in the deep saturation area.

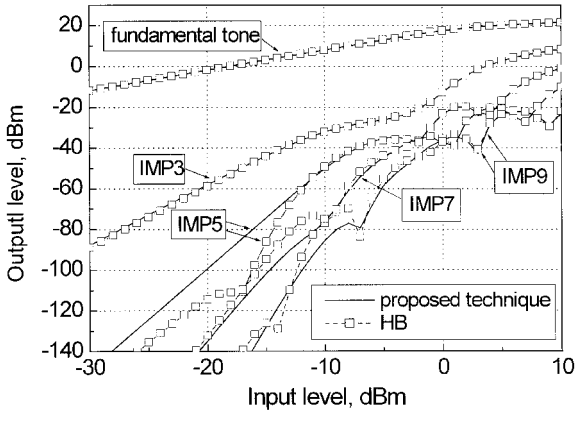

Figure 11. Fundamental tone, and third to ninth odd-order IMPs at the amplifier output versus input level.

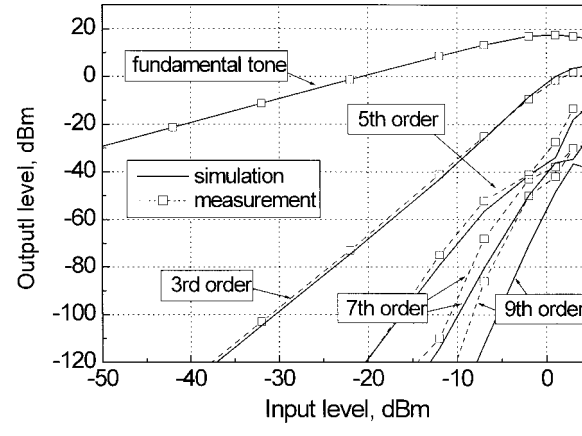

Figure 13. Fundamental, and third to ninth odd harmonics at the amplifier output versus input level.

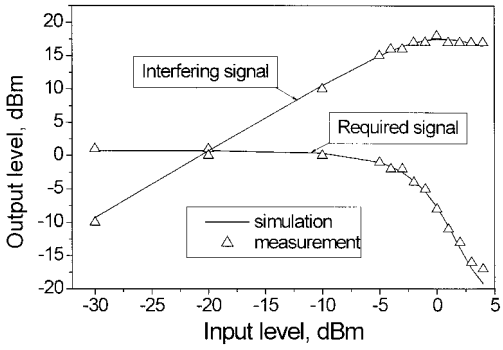

Figure 14. Desensitization in the amplifier: required and interfering signals at the output versus interfering signal at the input (the required signal amplitude at the input is fixed).

7. CONCLUSION

In this paper, we have presented the instantaneous quadrature technique as an efficient tool for behavioral-level simulation of RF/microwave circuits and systems. This technique combines the advantages of both the quadrature modeling technique and the discrete technique and, consequently, gives one possibility to simulate the circuit nonlinear performance over wide frequency and dynamic ranges (i.e., to predict harmonics and even-order nonlinear products, to simulate multicarrier systems, and to take into account the bias decoupling network effect) taking into account both AM–AM and AM–PM nonlinearities in a computationally efficient way. Even-order IMPs can be predicted as well. However, in order to get accurate results, one needs to measure or simulate AM–AM and AM–PM accurately (especially for second-order characteristics). The transformation of the envelope transfer functions into instantaneous ones was considered in detail, including numerical as well as analytical techniques.

Let us note some possible applications of the instantaneous quadrature technique:

1. Simulation of power amplifiers of wireless communication systems (this is the widest and most popular application).
2. Simulation of the entire transmitting path (not only the power amplifier, but also modulators, frequency multipliers, etc.) with viewpoint of nonlinear interference and distortion.
3. Simulation of a receiving path (low-noise amplifiers, mixers, intermediate frequency amplifiers, detectors, etc.) with viewpoint of nonlinear interference and distortions and EMC/EMI problems.
4. Previous items suggest that the nonlinear simulation of the entire communication link is possible (for example, the simulation of cellular communication system in order to predict interference and distortions during the phase of frequency planning, or in order to estimate the performance of a modulation scheme or a signal processing technique).
5. Nonlinear modeling and simulation of active array antennas is also an important application [48, 67].

In the second part of this paper, we are going to consider in detail approximation/representation of AM–AM and AM–PM characteristics and instantaneous transfer factors (with viewpoint of the simulation accuracy), the choice of the sample points number (to discretize the integral equations), the simulation of amplitude, frequency, and phase detectors, and the identification of nonlinear interference/distortion (IMPs, harmonics, etc.) sources.

ACKNOWLEDGMENTS

The authors would like to thank Professor F. Gardiol, Professor V. Mordachev, Mr. J. Staudinger, and Mr. I. Cheremisinov for many helpful discussions, Mr. J. F. Zurcher for help with measurements, and Mr. O. Kashanskii for technical assistance. The financial support of this work by the Swiss Government is also appreciated.

REFERENCES

1. M.C. Jeruchim, P. Balaban, and K.S. Shanmugan, Simulation of communication systems, Plenum Press, New York, 1992.
2. W.H. Tranter and K.L. Kosbar, Computer-aided design and analysis of communication systems, in The electrical engineering handbook, CRC Press, Boca Raton, FL, 1993, pp. 1593–1609.
3. F.M. Gardner and J.D. Baker, Simulation techniques: Models of communication signals and processes, Wiley, New York, 1997.
4. Special issue on computer-aided modeling, analysis and design of communication systems, IEEE J Selected Areas Commun 2(1) (1984), 8–203.
5. Special issue on computer-aided modeling, analysis and design of communication systems II, IEEE J Selected Areas Commun 6(1) (1988), 5–125.

6. Special issue on computer-aided modelling, analysis and design of communication links, IEEE Trans Selected Areas Commun 15(4), May 1997.
7. A.F. Peterson, S.L. Ray, and R. Mittra, Computational methods for electromagnetics, IEEE Press, New York, 1998.
8. T. Itoh and B. Haushmand (Eds.), Time-domain methods for microwave structures: Analysis and design, IEEE Press, New York, 1998.
9. Special issue on advanced numerical techniques in electromagnetics, IEEE Trans Antennas Propagation 45(3) (1997), 313–572.
10. S.M.S. Imtiaz and S.M. El-Ghazaly, Global modeling of millimeter-wave circuits: electromagnetic simulation of amplifiers, IEEE Trans Microwave Theory Tech 45(12) (1997), 2208–2216.
11. G.F. Carey, W.B. Richardson, C.S. Reed, B.J. Mulvaney, Circuit, Device and Process Simulation, New York, Wiley & Sons, 1996.
12. T.A. Fjeldly, T. Ytterdal, and M. Shur, Introduction to device modeling and circuit simulation, Wiley, New York, 1998.
13. J. Vlach and K. Singhal, Computer methods for circuit analysis and design, Van Nostrand Reinhold, New York, 1994.
14. M.B. Steer, C. Chang, and G. Rhyne, Computer-aided analysis of nonlinear microwave circuits using frequency-domain nonlinear analysis techniques: the state of the art, Int J Microwave Millimeter-Wave CAE 1(2) (1991), 181–200.
15. R.J. Gilmore and M.B. Steer, Nonlinear circuit analysis using the method of harmonic balance—a review of the art. Part I. Introductory concepts, Int J Microwave Millimeter-Wave CAE 1(1) (1991), 22–37.
16. R.J. Gilmore and M.B. Steer, Nonlinear circuit analysis using the method of harmonic balance—a review of the art. Part II. Advanced concepts, Int J Microwave and Millimeter-Wave CAE 1(2) (1991), 159–180.
17. V. Rizzoli, A. Lipparini, A. Costanzo, F. Mastri, C. Cecchetti, A. Neri, D. Masotti, State-of-the-art harmonic balance simulation of forced nonlinear microwave circuits by the piecewise technique, IEEE Trans Microwave Theory Tech 40(1) (1992), 12–28.
18. J.F. Sevic, M.B. Steer, and A.M. Pavio, Nonlinear analysis methods for the simulation of digital wireless communication systems, Int J Microwave Millimeter-Wave CAE 6(3) (1996), 197–216.
19. S.W. Chen, W. Panton, and R. Gilmore, Effects of nonlinear distortion on CDMA communication systems, IEEE Trans Microwave Theory Tech 44(12) (1996), 2743–2750.
20. F. Gagnon, N. Batani, R. Bourdeau, J. Belzile, On a complete simulation model for the design of high-speed digital radios, IEEE J Selected Areas Commun 15(4) (1997), 685–693.
21. M.I. Sobhy, E.A. Hosny, M.W.R. Ng, and E.A. Bakkar, Nonlinear system and subsystem modeling in time domain, IEEE Trans Microwave Theory Tech 44(12) (1992), 2571–2579.
22. R.F. Milson, P.A. Jamieson, and K.J. Scott, EMI prediction in system level simulation, 11th Int Zurich EMC Symposium, Zurich, Switzerland, 1995, pp. 215–220.
23. R. Saleh, S.-Jye Jou, and A.R. Newton, Mixed-mode simulation and analog multilevel simulation, Kluwer, Boston, 1994.
24. S. Ooms and D. DeZutter, The anti-circuit concept for the characterization of active circuits using electromagnetic simulations, IEEE Trans Microwave Theory Tech 44(11) (1996), 2032–2038.
25. Q. Chen and V.F. Fusco, Combined EM field/linear and nonlinear circuit simulation using the FDTD method, IEE Proc—Microwaves, Antennas Propagation 145(2) (1998), 185–189.
26. J.W. Bandler, R.M. Biernacki, S.H. Chen, P.A. Grobelny, Optimization technology for nonlinear microwave circuits integrating electromagnetic simulations, Int J Microwave Millimeter-Wave CAE 7(1) (1997), 6–28.
27. C.N. Kuo, B. Houshmand, and T. Itoh, Full-wave analysis of packaged microwave circuits with active and nonlinear devices: an FDTD approach, IEEE Trans Microwave Theory Tech 45(5) (1997), 819–826.
28. E. Larique, S. Mons, D. Baillargeat, S. Verdeyme, M. Aubourg, P. Guillon, R. Quere, Electromagnetic analysis for microwave FET modeling, IEEE Microwave Guided Wave Lett 8(1) (1998), 41–43.
29. A.R. Kaye, D.A. George, and M.J. Eric, Analysis and compensation of bandpass nonlinearities for communications, IEEE Trans Commun 20(11) (1972), 965–972.
30. J.S. Kenney and A. Leke, Power amplifier spectral regrowth for digital cellular and PCS applications, Microwave J 38(10) (1995), 74–90.
31. J. Staudinger, Applying the quadrature modeling technique to wireless power amplifiers, Microwave J 40(11) (1997), 66–86.
32. J. Staudinger, Behavioral analysis method applied to the design and simulation of linear power amplifiers, RAWCON'98 Workshop Modeling and Simulation of Devices and Circuits for Wireless Communications, Colorado Springs, CO, 1998.
33. G. Chrisikos, C.J. Clark, A.A. Moulthrop, M.S. Muha, C.P. Silva, A nonlinear ARMA model for simulating power amplifiers, IEEE MTT Symp Digest, Baltimore, MD, 1998, pp. 733–736.
34. K. Horiguchi, K. Yamauchi, K. Mori, N. Nakayama, T. Takagi, A novel distortion analysis method for amplifiers considering frequency characteristics, IEEE MTT Symp Digest, Baltimore, MD, 1998, pp. 1619–1622.

35. V. Borich, J.H. Jong, J. East, W.E. Stark, Nonlinear effects of power amplification on multicarrier spread spectrum systems, IEEE MTT Symp Digest, Baltimore, MD, 1998, pp. 323–326.
36. M.S. Muha, C.J. Clark, A.A. Moulthrop, C.P. Silva, Validation of power amplifier nonlinear block models, IEEE MTT Symp Digest, Anaheim, CA, 1999, pp. 759–762.
37. V.I. Mordachev, Applying the fast fourier transform for the analysis of nonlinear phenomena in radio receivers and amplifiers, Tech Mem 822BE-D83, VINITI, Moscow, 1983 (in Russian).
38. V.I. Mordachev, Express-analysis of unintended radio interference in severe electromagnetic environment using fast Fourier transform, Conf on Development and Implementation of Modern Radio Receiver Technology, Radio i Sviaz, Moscow, 1985 (in Russian).
39. V.I. Mordachev, Development of the algorithms for the analysis of unintended radio interference in a radio-receiving path in a given electromagnetic environment, Tech Rep 16/87, Minsk, Belarus, 1987 (in Russian).
40. V.I. Mordachev, RF signal discretization noise during the discrete modeling of a radio-receiving path, Tech Rep 271/88, Minsk, Belarus, 1988 (in Russian).
41. V.I. Mordachev, Express analysis of electromagnetic compatibility of radio electronic equipment with the use of the discrete models of interference and fast Fourier transform, Proc IX Int Wroclaw Symp on EMC, Poland, Wroclaw, 1988, part 2, pp. 565–570.
42. V.I. Mordachev, Software for the simulation of unintended RF interference in complicated electromagnetic environment, Tech Rep 19/88, Minsk, Belarus, 1988 (in Russian).
43. O.M. Ivanov, S.L. Loyka, V.I. Mordachev, and S.Yu. Shepurev, Radioreceiver functional modeling for electromagnetic compatibility express-analysis, Proc Int Conf Susceptibility and Electromagnetic Compatibility. Design and Certification Methods (EMCS-93), Minsk, Belarus, 1993, pp. 28–32 (in Russian).
44. S.L. Loyka and V.I. Mordachev, Computer-aided nonlinear simulation at the system level, Proc 5th Int Conf on Electromagnetic Interference and Compatibility (INCEMIC'97), Hyderabad, India, 1997, pp. 93–98.
45. S.L. Loyka and V.I. Mordachev, Mathematical models and algorithms of electromagnetic compatibility analysis and prediction software complex, Tech Rep 1(2), Belorussian State University of Informatics and Radioelectronics, Minsk, Belarus, 1997.
46. S.L. Loyka and V.I. Mordachev, Identification of nonlinear interference sources with the use of the discrete technique, IEEE Int Symp Electromagnetic Compatibility, Denver, CO, 1998, pp. 882–887.
47. S.L. Loyka, Detector simulation with the use of the discrete technique, 14th Int Wroclaw Symp on Electromagnetic Compatibility, Poland, Wroclaw, 1998, pp. 311–315.
48. S.L. Loyka, The influence of electromagnetic environment on operation of active array antennas: Analysis and simulation techniques, IEEE Antennas Propagation Mag, 41(6) (1999), 23–39.
49. S.L. Loyka, Numerical simulation of nonlinear interference in radio systems (invited paper), 26th URSI General Assembly, Toronto, Canada, 1999.
50. W.H. Press, B.P. Flanneay, S.A. Teukolsky, and W.T. Vetterling, Numerical recipes in *C*, Cambridge University Press, 1988.
51. V.I. Petko, V.E. Kukonin, and N.B. Shilov, Digital filtering and signal processing, Universitetskoe, Minsk, Belarus, 1995 (in Russian).
52. Q.H. Liu and X.Y. Tang, Iterative algorithm for nonuniform inverse fast Fourier transform (NU-IFFT), Electron Lett, 34(20) (1998), 1913–1914.
53. Q.H. Liu and N. Nguyen, An accurate algorithm for nonuniform fast Fourier transforms (NUFFT's), IEEE Microwave Guided Wave Lett 8(1) (1998), 18–20.
54. N. Suematsu, Y. Iyama, and O. Ishida, Transfer characteristic of IM_3 relative phase for a GaAs FET amplifier, IEEE Trans Microwave Theory Tech 45(12) (1997), 2509–2514.
55. Advanced design system, Hewlett-Packard Company, Santa Rosa, CA, 1998.
56. S.L. Loyka and I.D. Cheremisinov, Validation of the high-order polynomial models used in behavioral-level simulation, 4th Int Conf on Telecommunications in Modern Satellite, Cable and Broadcasting Services, Nis, Yugoslavia, 1999, pp. 592–595.
57. N.N. Blachman, Detectors, bandpass nonlinearities, and their optimization: inversion of the Chebyshev transform, IEEE Trans Information Theory 17(4) (1971), 398–404.
58. I.D. Cheremisinov and S.L. Loyka, Calculation of the instant transfer factor using the first and second order amplitude characteristics, Proc Belarus Engineering Academy 2 (1998), 57–60 (in Russian).
59. I.D. Cheremisinov, S.L. Loyka and V.I. Mordachev, Synthesis of the polynomial model of nonlinear elements based on intermodulation dynamic ranges, Proc 3rd Int Conf on Telecommunications in Modern Satellite, Cable and Broadcasting Services (TELSIKS'97), Nis, Yugoslavia, 1997, pp. 519–522.
60. I.D. Cheremisinov and S.L. Loyka, 2D polynomial models of mixers and analog multipliers for discrete EMC analysis, Int Conf on New Information Technologies for Science and Industry, Minsk, Belarus, 1998 (in Russian).
61. I.D. Cheremisinov and S.L. Loyka, Polynomial models of radio system nonlinear stages for the discrete EMC analysis, 8th Int Crimean Conf Microwave & Telecommunications Technology (CriMiCo 98), Crimea, Ukraine, 1998, pp. 408–409.

62. I.D. Cheremisinov and S.L. Loyka, Estimation of FFT aliasing impact on the accuracy of discrete EMC analysis, Int Conf on New Information Technologies for Science and Industry, Minsk, Belarus, 1998 (in Russian).
63. F.J. Harris, On the use of windows for harmonic analysis with the discrete Fourier transform, Proc IEEE 66(1), 1978, 51–83.
64. L.A. Vanstein and D.E. Vakman, Frequency separation in the theory of oscillations and waves, Nauka, Moscow, 1983 (in Russian).
65. L.M. Fink, Signals, interference, errors . . . , Radio i Sviaz, Moscow, 1984 (in Russian).
66. S.L. Loyka, On accuracy of numerical EMC/EMI modeling over a wide frequency range, Int Symp on EMC (EMC'98 Roma), Rome, Italy, 1998, pp. 684–688.
67. J.J. Schuss, J. Upton, B. Myers, T. Sikina, A. Rohwer, P. Makridakas, R. Francois, L. Wardle, R. Smith, The IRIDIUM main mission antenna concept, IEEE Trans Antennas Propagation 47(3) (1999), 416–424.

BIOGRAPHIES

Sergey L. Loyka was born in Minsk, Republic of Belarus on August 6, 1969. He received the M.S. degree with honors from Minsk Radioengineering Institute, Minsk, Republic of Belarus in 1992 and the Ph.D. degree in Radio Engineering from the Belorussian State University of Informatics and Radioelectronics, Minsk, Republic of Belarus in 1995.

Since 2000 he has been a postdoctoral fellow in the Laboratory of Communications and Integrated Microelectronics (LACIME) of Ecole de Technologie Superieure, Montreal, Canada. From 1995 to 2000 he was a senior researacher at the Electromagnetic Compatibility Laboratory, Belorussian State University of Informatics and Radioelectronics, Minsk, Belarus. From 1998 to 1999, he was an invited scientist at the Laboratory of Electromagnetism and Acoustic, Swiss Federal Institute of Technology, Lausanne, Switzerland.

Dr. Loyka is a member of the New York Academy of Sciences and of the IEEE. He has over 70 publications in the area of nonlinear RF/microwave circuit and system modeling and simulation, active array antennas, and electromagnetic compatibility. He received a number of awards from the USRI, the IEEE, the Swiss, Belarus, and former USSR governments, and the Soros Foundation.

Juan R. Mosig was born in Cadiz, Spain. He received the Electrical Engineer degree in 1973 from Universidad Politecnica de Madrid, Spain. In 1976 he joined the Laboratory of Electromagnetics and Acoustics at Ecole Polytechnique Fédérale de Lausanne (EPFL), Switzerland, from which he obtained a Ph.D. degree in 1983. Since 1991 he has been a professor at EPFL and since 2000 the Director of the Laboratory of Electromagnetics and Acoustics. In 1984, he was a Visiting Research Associate at Rochester Institute of Technology, Rochester, NY. He has also held scientific appointments at the universities of Rennes (France), Nice (France), Technical University of Danemark, and University of Colorado at Boulder, CO, USA. Dr. Mosig is the author of four chapters in books on microstrip antennas and circuits. He is co-organizer and lecturer of yearly, short intensive courses in Numerical Electromagnetics (Europe and USA). He is a member of the Swiss Federal Commission for Space Applications responsible for several research projects for the European Space Agency. His research interests include electromagnetic theory, numerical methods and microstrip antennas. He is a Fellow of the IEEE.